conferenceseries.com
www.conferenceseries.com

37th Global Nanotechnology Congress

October 21-22, 2020 | Frankfurt, Germany

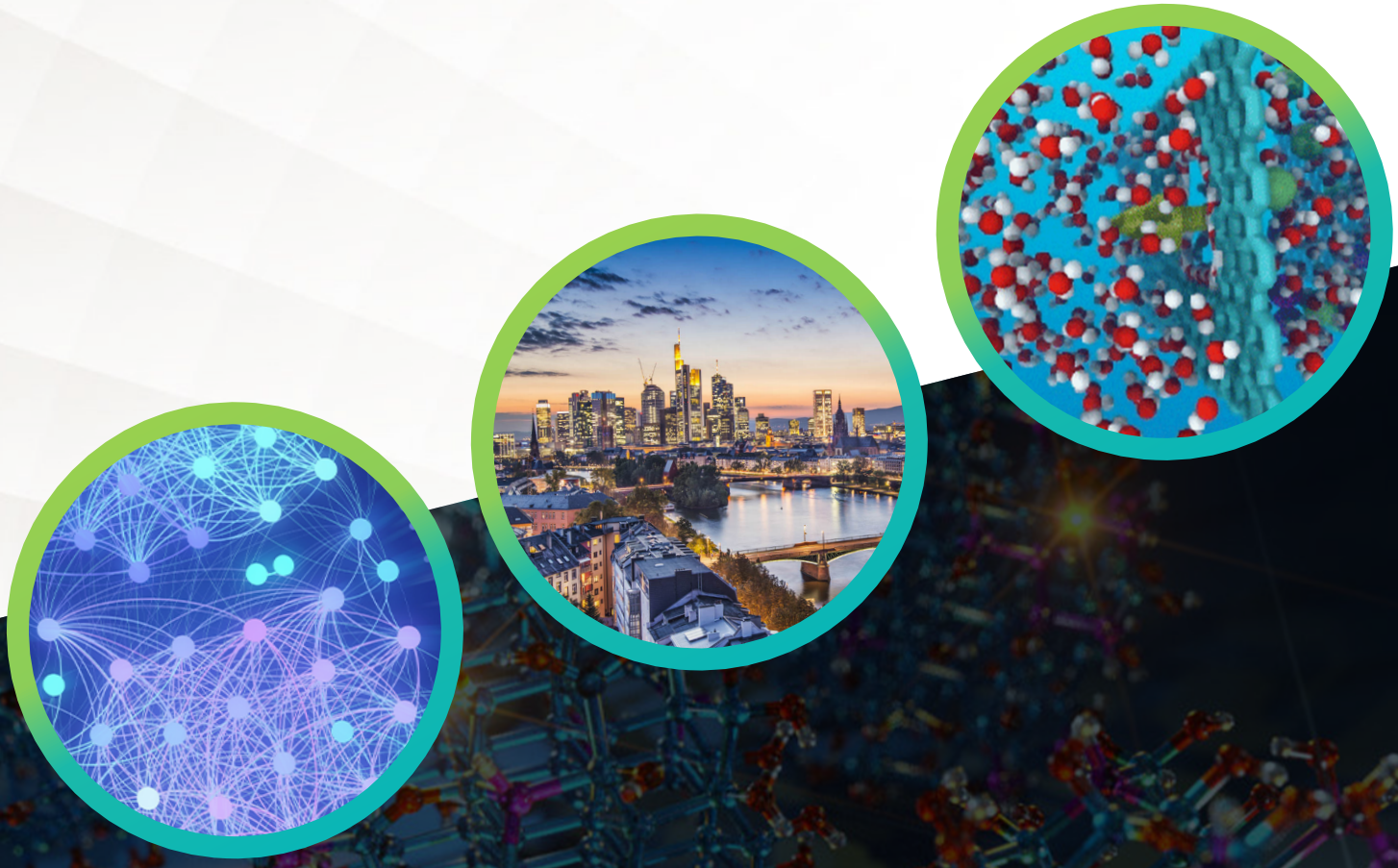

+44 7460854031

SCIENTIFIC PROGRAM

SCIENTIFIC PROGRAM

Wednesday, 21st October 2020

DAY 1

08:30-09:00	Registrations
09:00-09:30	Introduction
09:30-09:50	COFFEE BREAK
09:50-11:50 Meeting Hall 01	Keynote LECTURES

	MEETING Hall 01	MEETING Hall 02
11:50-13:10	Talks On: Gastroenterology and Hepatology	Talks On: Advances in Gastrointestinal Treatments
	Gastroenterology	Gastrointestinal Bleeding and Pathology
	Gastrointestinal Infection	Advances in Gastrointestinal Endoscopy
	Colorectal and Intestinal Disorders	Esophageal Diseases

13:10-13:15	GROUP PHOTO
13:15-14:00	LUNCH BREAK

	MEETING Hall 01	MEETING Hall 02
14:00-16:00	Talks On: Gallstones and Bile Duct Stones	Talks On: Gastroparesis
	Advanced Materials and Functional Devices	Magnetism and Multiferroism
	Engineering Materials	Optical Materials and Plasmonics
	Composite Materials	Energy and Harvesting Materials

16:00-16:20	COFFEE BREAK

MEETING Hall 01 (16:20-17:00)	MEETING Hall 01 (17:00-18:00)
Nanotechnology-Basics to Applications	Carbon Nanostructures and Graphene
Nano Materials	Spintronics
Nano Structures	Nanoparticle Synthesis and Applications
Properties of Nano Materials	

37th Global Nanotechnology Congress

October 21-22, 2020 Germany **Webinar**

Latest Technologies and Innovative Concepts in the Field of Nanotechnology

Subject area: Carbon Nanostructures and Graphene

MULTIPLE-WALL CARBON NANOTUBES OBTAINED WITH MESOPOROUS MATERIAL DECORATED WITH CERIO-ZIRCONIUM

Oscar A. Anunziata, María L. Martínez*

Centro de Investigación en Nanociencia y Nanotecnología (NANOTEC), Facultad Regional Córdoba, Universidad Tecnológica Nacional, Maestro y Cruz Roja Argentina, (5016), Córdoba, Argentina.

Keywords: Nanotubes; Ce-Zr-SBA-15; CVD; Synthesis; Characterization

ABSTRACT

In this work, Ce-Zr-SBA-15 has been used directly as a catalyst for the synthesis of multi-vall carbon nanotubes (MWCNT) through Chemical Vapor Deposition (CVD). In addition to cerium oxide, it contains zirconium oxide Nano crystallites, which act as catalysts for carbon nanostructures. The catalytic performance of this material was evaluated for the decomposition of ethanol at 900 °C, with N_2 flow. The structural characterization of the resulting catalyst was carried out by means of SEM and XRD. The decomposed carbon of absolute ethanol diffuses through the surface of the nanostructured material and precipitates in carbon structures called multiple-walled nanotubes, which could be visualized/detected/identified by TEM, showing diameters of the carbon nanotubes that range from 15 to 25 nm.

1. INTRODUCTION

In the past two decades, carbon nanotubes (CNTs) have been the target of extensive research due to their uniqueness and incomparable physicochemical properties [1, 2] and their possible applications in nanoscience and nanotechnology. Examples include electronics [3–5], high-strength polymer compounds [6, 7], high-resolution imaging nanoprobes [8] and hydrogen storage [9]. This technological relevance gave rise to intensive research activity on catalytic chemical vapor deposition (CVD), which has been widely considered for the large-scale synthesis of CNT [10, 11] of the decomposition of various hydrocarbons using transition metals as catalysts in different metals and oxide supports [12]. Unfortunately, large-scale production of CNT through catalytic CVD is still expensive. Actually, in addition to the availability of the carbon source, the main cost factors derive from the preparation of substrates (such as silicates or aluminates), as well as the finely dispersed diffusion of metallic particles (Fe, Ni or Mg) on them. In the present work, we have been able to develop multiple-walled carbon nanotubes by chemical deposition of ethanol vapor and low nitrogen flow on a cerium and zirconium species deposited on the mesoporous material SBA-15.

2. EXPERIMENTAL

2.1 Ce-Zr-SBA-15 Preparation The synthesis of the ordered mesoporous silica SBA-15 was made according to previous work [13]. Cerium and zirconium were incorporated into the Si-SBA-15 support by the wet co-impregnation method for the bimetal catalyst. The metallic precursors used were cerium (III) nitrate hexahydrate (99% from Aldrich) as the source of Ce and hydrated zirconium

oxychloride (99.99%, Aldrich) as the source of Zr. The precursor salts were dissolved in 10 mL of ethanol to obtain molar ratios of Si / (Ce + Zr) = 20 in the final solid. A finely ground powder fraction (1 g) of the SBA-15 was dried in static air at 100 °C for 12 h, then directly incorporated into the cerium and zirconium solution. The solution was placed on a rotary evaporator to remove excess ethanol at approximately 80 °C and 80 rpm. The resulting material was then dried at 100 °C for 24 h and heat treated in a dynamic inert atmosphere (N_2) with a heating rate of 4 °C / min at 470 °C for 5 h. The sample was then calcined at 500 °C of air for 5 h. The catalyst is called Ce-Zr-SBA-15.

2.2 Synthesis of carbon nanotubes

The synthesis was carried out by the Chemical Vapor Deposition (VCD) technique, using a carbon source, vaporizing it or introducing it into a transport gas, so that it came into contact with the catalyst. Under high temperature conditions, it is possible to carry out the reaction of formation of carbon nanotubes on the metal oxide clusters. Ethanol was used as a carbon source. The catalytic material is the mesoporous structure synthesized for this purpose and functionalized (Ce-Zr-SBA-15). The reaction conditions are detailed below: the working temperature was 900 °C; under these reaction conditions, a quartz reactor with a diameter of 10 mm and a length of 600 mm was used, with a reaction time of 30 min.

2.3 Characterization

XRD analysis were recorded with a Rigaku X-ray diffractometer system (RINT-2200) with CuK α radiation (1.5406 Å) and a nickel filter. BET surface area analyzer (Quantachrome / Autosorb1) analyzed the isotherms and texture properties. SEM micrographs were obtained using JEOL JSM-6610LV. XPS were acquired on a Microtech Multilb 3000 spectrometer, equipped with a hemispherical electron analyzer and MgKα (hv=1253.6 eV) photon source. TEM micrographs of MWCNT were acquired in a JEOL microscope model JEM-1200 EX II.

3. RESULTS AND DISCUSSION

3.1 XRD

Figure 1 shows the low-angle X-ray diffraction pattern. We can see three diffraction peaks corresponding to planes (100), (110) and (200) of the ordered 2D p6mm hexagonal pore structure typical of SBA-15 used as a reference [14]. The main peak at 2θ = 0.82-0.87° corresponds to the first plane (100) attributed to the presence of regular intermediate spaces between the walls of the mesoporous channels. In addition to the other two additional peaks, long-range ordered pores seem to be preserved in the sample. Compared to the SBA-15 support (not shown in the figure), in the synthesized sample we observed attenuation in the intensity of the main peak and its maximum shifted slightly to higher 2θ after addition of Ce and Zr species, indicating some decrease in both 100 spaces and mesopore diameters [15]. This implies that the metal oxides are embedded in the nanochannels and dispersed on the surface, without affecting the structural order of the SBA-15 support.

The inset figure shows high-angle diffraction patterns of the catalytic material. The crystalline phase of ZrO_2 was not found in any catalyst, suggesting that Zr species are well dispersed in the mesoporous structure. In contrast, cerium oxide has measurable crystallites. The diffraction angles of the cerium oxide reference phases are present in these catalysts. The 2θ peaks of 28.6 °, 33.2 °, 47.4 °, 56.4 °, 59.1 °, 69.4 °, 76.8 ° and 79.1 ° in the sample refer to the diffraction planes (111), (200), (220), (311), (222), (400), (331) and (420) characteristic of the fluorite CeO_2 phase (cubic CeO_2 planes with fluorite structure (Fm3m, JCPDS: 43–1002)). The presence of crystalline CeO_2 in these catalysts indicates that the Ce is not well dispersed in the mesoporous structure of the catalyst. The size of the cerium oxide particles was determined using the Scherrer formula [16] and the value obtained was 6.0 nm for Ce-Zr-SBA-15.

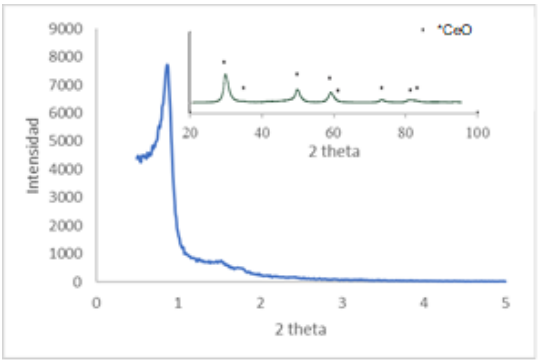

Figure 1: Ce-Zr-SBA-15 XRD at low angle, inset: XRD at high angle

3.2 BET-SEM of Ce-Zr-SBA-15

Table 1 and Figure 2(a) shows the analysis of nitrogen absorption-desorption isotherms of the catalyst. The sample has a typical type IV isotherm with H1 type hysteresis cycle, typical of the SOP-15 mesoporous structure. When Ce and Zr are incorporated into the sample, the hysteresis cycle is briefly altered, presenting a relative pressure range (P / Po) of 0.4–0.8, as shown in Fig. 2, while SBA-15 is generally seen in the P/Po region of 0.6-0.8 [17]. This suggests some irregularities in the porous system that could indicate that Ce and Zr oxides are partially blocking mesopores.

Table 1: Textural properties of the catalyst

Samples	Surface area (m^2/g)	Average pore diameter (nm)	Pore Volume (cm^3/g)
SBA-15	880	8.10	1.20
Ce-Zr-SBA-15	465	5.60	0.65

Table 1 summarizes the physicochemical and textural properties of the samples synthesized. The Ce-Zr-SBA-15 mesoporous material has lower surface area, pore volume, and pore size compared to pure SBA-15 used as a reference.

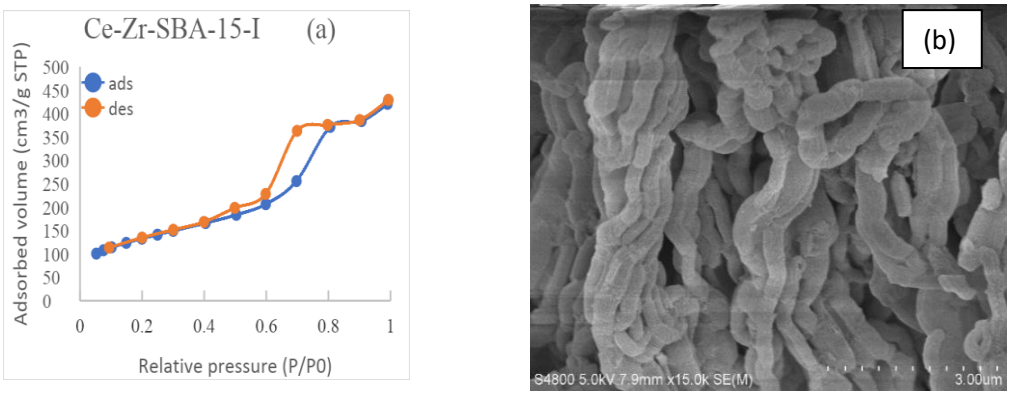

Figure 2: (a) BET isotherm, (b) SEM microscopy of Ce-Zr-SBA-15 catalysts

The addition of cerium plus zirconium significantly reduced surface area [15], indicating the incorporation of Ce-Zr oxide particles in the mesoporous structure. Figure 2 (b) shows that the catalyst has the typical fibrous morphology and long mesochannels (1.0–1.5μm) corresponding to SBA-15. The morphology of the samples prepared by direct synthesis is slightly different from that of the impregnated samples. This could be due to the agglomeration of the crystals by the new and successive heat treatments after impregnation.

3.3 XPS analysis

Using XPS, we investigated the interactions between silica oxide and ceria-zirconia oxides. Table 2 provides the electron binding energies (BE) of Zr $3d_{5/2}$ and $3d_{3/2}$, Ce $3d_{5/2}$ and $3d_{3/2}$ signal for different species.

Table 2: XPS parameters from Ce-Zr-SBA-15 catalyst

Sample	Species	BE (eV)	Species	BE (eV)
		Zr $3d_{5/2}$ and $3d_{3/2}$		Ce $3d_{5/2}$ and $3d_{3/2}$
Ce-Zr-SBA-15	ZrO_2	182.56	Ce_2O_3	886.1
				904.34
	$ZrSiO_4$	183.68	CeO_2	916.62

We can observe that Zr exist in their maximum oxidation states (+ 4). The Ce 3d spectra show abundant states that result from the different occupations of the Ce 4d level in its final state, exhibiting binding energy values consistent with those reported in the literature [15].

3.4 TEM-SEM MWCNT

Figure 3 shows the image acquired by TEM and SEM microscopy of carbon nanotubes.

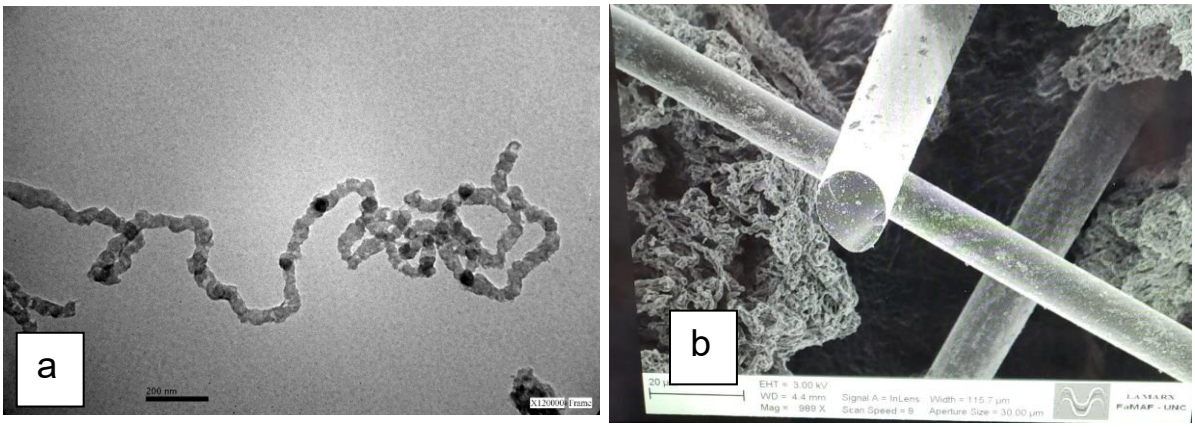

Figure 3: TEM (a) and SEM (b) microscopy of carbon nanotubes created

According to TEM Image, the diameter of the nanotubes ranges from 15 to 25 nm. It can also be seen that these nanotubes have nodes (darker points in the image) produced during the synthesis process due to their superficial growth on the metal oxide particles. Nanotubes of different lengths (Fig. 3b) were obtained and some were perfectly linear while others were curved. The image shows

that there was a production of tubes with different diameters. Being the first and novel synthesis of MWCNT, the path continues in this investigation to achieve uniformity in its production.

CONCLUSIONS

Mesoporous SBA-15 material was synthesized and cerium and zirconium oxides were introduced by wet impregnation. Using different characterization techniques, we can conclude that the incorporation of these metals in the support introduced no significant changes. In this way when chemical vapor deposition was carried out, multiple-walled carbon nanotubes with diameters ranging from 15 to 25 nm were obtained. We have proven that using ethanol as a carbon source through CVD on Ce-Zr-SBA-15, catalytic material carbon nanotubes can be successfully obtained.

Acknowledgments

M.L. Martinez, O. A. Anunziata, NANOTEC, CONICET Researchers. We acknowledge the financial support of CONICET Argentina, PIP CONICET 11220120100218CO 2014–2018 and PICT-FONCyT RES 475/2015; 2017–2021.

REFERENCES

[1] P.M. Ajayan, Nanotubes from carbon, Chem. Rev. 99 (1999) 1787–1799.
[2] M.S. Dresselhaus, G. Dresselhaus, P.C. Eklund, Science of Fullerenes and Carbon Nanotubes, Academic Press, New York, 1996.
[3] S.J. Tans, A.R. Verschueren, C. Dekker, Room-temperature transistor based on a single carbon nanotube, Nature 393 (1998) 49–52.
[4] P.G. Collins, P. Avouris, Nanotubes for electronics, Sci. Am. 283 (2000) 38–45.
[5] S.J. Tans, M.H. Devoret, H. Dai, A. Thess, R.E. Smalley, L.J. Geerlings, C. Dekker, Individual single-wall carbon nanotubes as quantum wires, Nature 386 (1997) 474–477.
[6] P. Calvert, Nanotube composites: a recipe of strength, Nature 399 (1999) 210–211.
[7] H.D. Wagner, O. Lourie, Y. Feldman, R. Tenne, Stress-induced fragmentation of multiwall carbon nanotubes in a polymer matrix, Appl. Phys. Lett. 72 (1998) 188–190.
[8] H.J. Dai, J.H. Hafner, A.G. Rinzler, D.T. Colbert, R.E. Smalley, Nanotubes as nanoprobes in scanning probe microscopy, Nature 384 (1996) 147–150.
[9] A.C. Dillon, K.M. Jones, T.A. Bekkedahl, C.H. Kiang, D.S. Bethune, M.J. Heben, Storage of hydrogen in single-walled carbon, Nature 386 (1997) 377–379.
[10] C. Öncel, Y. Yürüm, Carbon nanotube synthesis via the catalytic CVD method: a review on the effect of reaction parameters, Fullerenes, Nanotubes and Carbon Nanostructures 14 (2006) 17–37.
[11] G.D. Nessim, Properties, synthesis, and growth mechanisms of carbon nanotubes with special focus on thermal chemical vapor deposition, Nanoscale 2 (2010) 1306–1323.
[12] M. Kumar, Y. Ando, Chemical vapor deposition of carbon nanotubes: a review on growth mechanism and mass production, J. of Nanosci. and Nanotech. 10 (2010) 3739–3758.
[13] J.Juárez, M.B. Gómez Costa, M.L. Martínez, O.A. Anunziata, Influence of vanadium nanoclusters in hydrogen uptake using hybrid nanostructured materials. J.Porous Mater. 26(2019)951–959.
[14] W.N. Wan Abdullah, W.A. Wan Abu Bakar, R. Ali, W.N.A. WanMokhtar, M.F. Omar,J. Clean. Prod. 162 (2017) 1455–1464.
[15] V. Shanmugam, R. Zapf, S. Neuberg, V. Hessel, G. Kolb, Appl. Catal. B-Environ. 203 (2017) 859–869.
[16] J.I. Langford, A.J.C. Wilson, J. Appl. Crystallogr. (1978) 11–102.
[17] F. Wang, J. Li, J. Yuan, X. Sun, J. Shen, W. Han, L. Wang, Catal. Commun. 12 (2011)1415–1419.